Multiple transformation analysis for interference separation in TDCS

WANG Guisheng [1,3,*], WANG Yequn [1,2], DONG Shufu [1], and HUANG Guoce [1]

1. Information and Navigation College, Air Force Engineering University, Xi'an 710077, China;
2. The 30th Research Institute of China Electronics Technology Corporation, Chengdu 610054, China;
3. National Key Laboratory of Airspace Technology Beijing 100192, China

Abstract: Various types of interference signals limit the practical application of transform domain communication systems (TDCSs) in the severe electromagnetic field, an orthogonal basis learning method of transformation analysis (OBL-TA) is proposed to effectively address the problem of obtaining an optimal transform domain based on sparse representation. Then, the sparse availability is utilized to obtain the optimal transformation analysis by the iterative methods, which yields the sparse representation for transform domain (SRTD) in unrestricted form. In addition, the iterative version of SRTD (I-SRTD) in unrestricted form is obtained by decomposing the SRTD problem into three sub-problems and each sub-problem is iteratively solved by learning the best orthogonal basis. Furthermore, orthogonal basis learning via cost function minimization process is conducted by stochastic descent, which is assured to converge to a local minimum at least. Finally, the optimal transformation analysis is developed by the effectiveness of different transform domains according to the accuracy of the sparse representation and an optimal transformation analysis separately (OPTAS) is applied to the synthesized signal forms with conic alternatives, dualization, and smoothing. Simulation results demonstrate that the superiorities of the proposed methods achieve the optimal recovery and separation more rapidly and accurately than conventional methods.

Keywords: transformation analysis, interference separation, sparse representation, transform domain communication system (TDCS).

1. Introduction

Ensuring a low probability of interception (LPI) and susceptibility to interference is essential for maintaining the security and reliability of communication in tactical operations. However, it is well known that the communication links are highly vulnerable to electromagnetic interference. This has been addressed in recent years by the development of cognitive communication [1,2]. These systems have been demonstrated to facilitate the mitigation of interference from perspectives of the transmitter and receiver simultaneously rather than the receiver only, which provides the capability of avoiding spectral bands occupied by interference sources or jammers. Furthermore, the cognitive framework enables the intelligent utilization of available frequency in the scarce spectrum under the complex and confrontational condition and the communication system synthesizes the adaptive anti-jamming waveforms for high spectrum efficiency through frequency pool nulling and spectral broadening via transformation analysis. Hence, the framework of cognitive communication systems is highly attractive for anti-jammer applications [3−5].

As one of the most common representatives in cognitive communication systems, the overall implementation of transform domain communication system (TDCS) first involves a sensing determination of the spectrum of interference or jamming signals, which is typically conducted by spectrum estimation techniques. Then, the surrounding signals are identified with transformation analysis in various domains and a fundamental modulation waveform (FMW) is created by a random basis function with various transform bases [6]. Because the FMW is spectrally synthesized to avoid the interfered regions, the transmitted energy cannot be injected into the interfered locations in the corresponding transformation analysis. Moreover, interference will affect the transmitted signals and anti-jamming performance diversely in different transformation analyses for both the transmitter and receiver. Meanwhile, communication performance can be further improved by applying the diverse range of avail-

able sparsity representations for distinguishing local signals and baleful signals. Therefore, obtaining the optimal transform domain for various interference signals under sparse representation is essential to ensure the security and reliability of communications in the TDCS.

The extensive development of signal processing theories promotes many novelties for transforming signals, such as the Fourier transform, fractional order Fourier transform, wavelet transform, and their derivatives [7–9]. More broadly, transformation analysis converts the detected signals into new representations using dimensionality reduction or feature extraction methods for principle component analysis (PCA) [10], linear discriminant analysis (LDA) [11], sparse learning [12,13], etc. And the transformation analysis is not necessarily restricted into linear transforms. However, the multiformity of signals and the presence of non-linear transform domains make the selection of the optimal transform domain difficult owing to the large amount of calculation involved. Additionally, the challenging task is particularly difficult to settle with the high cost and unreliability of large-scale training samples. Moreover, most of the existing methods rely on the manual and limited selection for particular signals, whereas actual signals are generally affected by many factors. Therefore, it is imperative to develop the transformation analysis methods that are flexibly applicable to general signals in order to broaden the practical applications.

This paper addresses the above-discussed issues by obtaining an optimal transform domain for various types of interference signals in the TDCS and an orthogonal basis learning method of transform analysis (OBL-TA) is proposed based on sparse representation. The process enables us to utilize the effectiveness of different transform domains to obtain the optimal transformation analysis for particular types of signals according to the accuracy of sparse representation based on the obtained orthogonal basis. Moreover, an optimal transformation analysis separately (OPTAS) is applied to the synthesized signal forms, which further improves the validity of interference classification and mitigation. The simulation results demonstrate that the proposed OBL-TA method obtains the optimal transform domain more rapidly and accurately than conventional methods, which illustrates the superiorities in effectiveness and timeliness. The primary contributions are summarized as follows.

(i) An OBL-TA is proposed, where the sparse representation of interference signals can be simplified based on the orthogonal basis obtained in the optimal transformation analysis.

(ii) The sparse representation for transform domain (SRTD) is obtained in unrestricted form, and an iterative version of SRTD (I-SRTD) is derived in unrestricted form, where the SRTD problem is decomposed into three sub-problems for the closed solutions.

(iii) Each sub-problem is solved by learning the best orthogonal basis and the flexible attenuation rate is alternated iteratively, where a cost function minimization process is conducted by stochastic descent.

(iv) An OPTAS is applied to the synthesized signal forms with conic alternatives, dualization and smoothing, which achieves the optimal transformation analysis according to the accuracy of sparse representation based on the separate characteristics for interference and sparse signals.

The rest of the paper is organized as follows. Section 2 describes the sparse representation for signals and derives the sparse representation for linear transform domains. In Section 3, the iterative optimization for general transformation analysis is proposed based on information entropy. Moreover, the optimal transformation analysis for synthesized signal forms is proposed in Section 4. Simulation results are presented in Section 5 and conclusions are given in Section 6.

2. Sparse representations for linear transform domains

In general, most signals processed in communication systems can be compressed by transforming them as a series of coefficients in some domains. However, many of the transform coefficients of natural signals are typically close to zero [14]. Accordingly, the compressed signals only occupy a small fraction of the transformed signal space, which may be represented sparsely by a few elementary components out of a given collection. Consequently, sparsity can also be observed in other classes of natural signals [15]. In fact, sparse signals are observed almost everywhere in the wide fields of signal processing and play an important role in a variety of tasks, such as radar imaging, interference characterization and data reduction. Accordingly, it is essential for the cognitive communication system to address these sparse signals in broadband spectrum.

2.1 TDCS signal

Different from direct sequence spread spectrum (DSSS) that mitigates interference at the receiver, the TDCS smartly synthesizes an adaptive waveform to avoid interference at the transmitter. The transmission sequence in TDCS has good autocorrelation and cross-correlation performance to achieve low LPI and orthogonality. Fig. 1 shows the processing steps of a general TDCS transmitter.
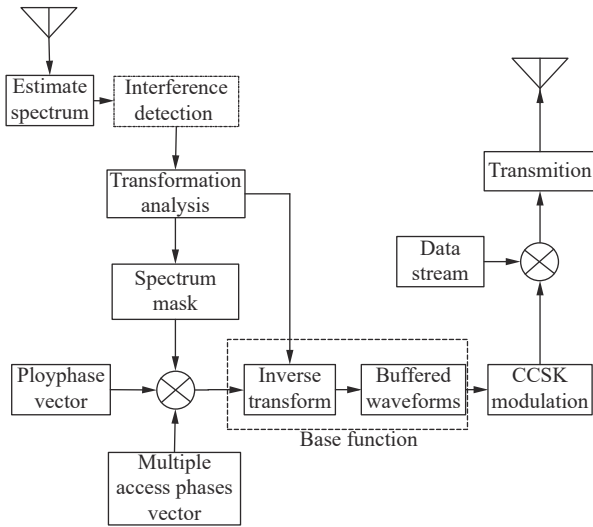
Fig. 1   Processing steps of a general TDCS transmitter

To ensure an interference-free transmission, a spectrum mask is determined by the magnitude shaping and the available spectrum. Among them, the complex polyphase vector is produced by a unique pseudorandom code selected randomly according to the spectrum mask and the phase space. Then, the mapping rules achieve the noise-like property of base function and the desired energy is distributed equally or diversely in the spectrum nulling to scale the magnitude. After selecting the optimal transformation analysis, the appropriate inverse transform is performed for the energy-injected waveforms to generate the buffered base function in the time domain. Generally, cyclic shift keying is utilized for modulation in TDCS to adapt noise-like properties. Finally, the information bit stream is synthesized by mapping the buffered base function and the transmitted waveform with the normalized energy factor.

It is a fact that the signal can be corrupted by additive Gaussian noise and external jamming when transmitted through the channel, the practical channels are mainly dominated by the line-of-sight (LOS) component and the possible limited multipath fade due to ground reflections where the propagation delay is mainly caused by path loss. Meanwhile, given the potentially relative mobility, Doppler frequency shifts may affect the channel, and consequently, the spectrum allocation.

When the length of the original signal is N, there are $W = 2^N$ possible forms of the transmitted signal in the entire signal space S. Only a small fraction of the space is occupied, which can be represented sparsely as

$$\begin{cases} s(t) = \Psi_T \theta_T \\ \Psi_T = [S_1, S_2, \cdots, S_W]^T \end{cases} \tag{1}$$

where Ψ_T is a sparse dictionary for signal space S and most coefficients θ_T are apparently equivalent to zero.

2.2   Interference analysis

In practice, the communication systems are subject to diverse types of interference in the complex environment and the multiform interference can be divided into three main categories, which include impulse interference, carrier interference and direct noise interference [16,17]. These latter two categories can be further divided as well. For example, the carrier interference occurs in many forms, such as sine, square, and saw-tooth waves, whereas the direct noise interference can be divided into different categories according to its modulation mode, such as amplitude modulation interference, frequency modulation (or phase modulation) interference and hybrid modulation interference [18]. Additionally, the above categories of interference can be divided generally based on their spectrum characteristics into targeted, multi-frequency and blocking interference categories. For instance, the narrow-band interference is representative of targeted interference [19,20]. Here, targeted interference typically represents interference with a high degree of similarity to the interfered signals. Multi-frequency interference interferes with multiple carriers, and is characterized as frequency-division, time-division, and comprehensive multi-frequency interference [21,22]. Among these, multi-tone interference is applied broadly to tactical communications. Blocking interference has the characteristics of wide broadband coverage, such as in the case of chirp interference and comb-spectrum interference. Considering the composition and application of jammer in practical applications, the Gaussian noise substituted for the interference source generator is investigated in this paper.

2.3   Sparse representation

Sparse representation is the basis of compressive sensing, which represents information in a signal as a small set of real or negative numbers and most of the coefficients are close to zero. To estimate the coefficients of sparse signals for representation where the interference or TDCS signals are defined as the general signal $x \in \mathbf{C}^N$, and $\mathbf{C}^N$ is regarded as the N-dimension complex vector. Consequently, the general signal x can be represented sparsely in the corresponding transform analysis T_*, which is formulated as

$$\begin{aligned} \min_{\Psi, \Theta} \quad & \|x - \Psi\Theta\|_F^2 \\ \text{s.t.} \quad & \|\Theta\|_0 \leqslant K \end{aligned} \tag{2}$$

where Ψ is a dictionary, which encodes the critical infor-

mation for a series of similar signals, $\boldsymbol{\Theta}$ is the coefficient vector, K is the sparsity, $\|\bullet\|_F$ denotes the Frobenius norm and $\|\bullet\|_0$ denotes the number of nonzero elements.

Efforts to design a suitable or general transform domain for signals began with the development of the Fourier transform, cosine transform and their derivatives [23]. Many pioneers have applied the fast Fourier transform (FFT) [24], fractional Fourier transform (FrFT) [8,25] and discrete wavelet or cosine transform (DWT/DCT) [26] for conducting signals decomposition and analysis. Because the diversities of signals include the time-varying and non-stationary characteristics, multiple transform domains have been applied for signal decomposition and analysis, such as the time domain, frequency domain, fractional domain and wavelet domain. These domains can be converted to each other and signals can be processed independently simultaneously.

In addition to dictionary learning methods, a signal may be sparse under a particular transformation whether the transformation is linear or whether the transformation matrix is reversible, such as in the case of gradient operators or curved shifts. Accordingly, the transformed signal is a sparse vector, and the transformation analysis $T_\bullet$ achieves the aforementioned transform domains for the general signal $\boldsymbol{x}$, satisfying the following condition:

$$\hat{T}_\bullet(\boldsymbol{x}) = \sum_{i=1}^{N} \psi_i \theta_i = \boldsymbol{\Psi}^{N\times N} \boldsymbol{\Theta}^{N\times 1} \tag{3}$$

where the sparsity $K \ll N$, ψ is a basis and θ denotes the projection coefficient vector.

According to iterative methods [27] with the fast gradient updating for α, sparse availability can be utilized to solve the problems in (2) and (3), the SRTD in unrestricted form [28] is given as

$$\min_{T_\bullet, \boldsymbol{\Psi}, \boldsymbol{\Theta}} \|T_\bullet(\boldsymbol{x}) - \boldsymbol{\Psi}\boldsymbol{\Theta}\|_F^2 + \alpha\|\boldsymbol{\Theta}\|_0 \tag{4}$$

where the attenuation rate is $\alpha > 0$.

In the simplest cases where the transformation analysis is restricted to linear transforms and $T_\bullet$ or $\boldsymbol{\Psi}$ is orthogonal, such as in the orthogonal base of the normalized DFT and various DWT, the matrix $T^{-1}\boldsymbol{\Psi}$ is invertible. The aforementioned problem in (4) can be simplified as

$$\min_{T^{-1}\boldsymbol{\Psi}, \boldsymbol{\Theta}} \left\|\boldsymbol{x} - T^{-1}\boldsymbol{\Psi}\boldsymbol{\Theta}\right\|_F^2 + \alpha\|\boldsymbol{\Theta}\|_0. \tag{5}$$

Therefore, the matrix $T^{-1}\boldsymbol{\Psi}$ can be obtained using a dictionary learning algorithm, such as the method of optimal directions (MOD) and k-singular value decomposition (kSVD), which is given by

$$\begin{cases} \boldsymbol{\Theta}^* = \underset{bm\theta_0 \leqslant k}{\arg\min} \left\|\boldsymbol{x} - T^{-1}\boldsymbol{\Psi}\boldsymbol{\Theta}\right\|_F^2 \\ [T^{-1}\boldsymbol{\Psi}]^* = \underset{T^{-1}\boldsymbol{\Psi}}{\min} \left\|\boldsymbol{x} - T^{-1}\boldsymbol{\Psi}\boldsymbol{\Theta}\right\|_F^2 + \alpha\|\boldsymbol{\Theta}\|_0 \end{cases}. \tag{6}$$

Once $T^{-1}\boldsymbol{\Psi}$ is obtained, it is easily factorized into an invertible matrix T^{-1} and an orthogonal matrix $\boldsymbol{\Psi}$ by matrix decomposition methods such as QR decomposition.

Naturally, solving the problem in (6) is computationally much simpler and cleaner than solving the problem in (4). Additionally, the complexity of the aforementioned approach for solving problem in (6) can be reduced from N^2 to $N\log_2 N$ by applying existing fast dictionary learning methods, where N is the dimensionality of interference signal $\boldsymbol{x}$. However, the transformation analysis often fails to conform to linear restrictions due to the multiformalism of signals involved and the nonlinearity of transform domains. Under these conditions, iterative optimization methods provide a means of an optimal solution to non-convex optimization problems.

3. General independent transformation analysis

Through converting the sparse signal to the appropriate domains for processing, the results have discovered obvious sparse features and many TDCS signals can be compressed, that is, they can express with sparse representations properly after transformation analysis by choosing appropriate basis, which pave the way to investigate the sparse representation and reconstruction further. Therefore, the sparse representation of the signal can be simplified to the orthogonal basis of the optimal transform domain.

The problem given in (4) can be simplified by decomposing it into the following three subproblems by temporarily fixing the variables. Then, it can be achieved by accelerating the process of optimization during iterations.

$$\begin{cases} \boldsymbol{\Theta}^* = \underset{\|\boldsymbol{\Theta}\|_0 \leqslant K}{\arg\min} \|T_\bullet(\boldsymbol{x}) - \boldsymbol{\Psi}\boldsymbol{\Theta}\|_F^2 \\ \boldsymbol{\Psi}^* = \underset{\boldsymbol{\Psi}}{\min} \|T_\bullet(\boldsymbol{x}) - \boldsymbol{\Psi}\boldsymbol{\Theta}^*\|_F^2 + \alpha\|\boldsymbol{\Theta}^*\|_0 \\ T_\bullet^*(\boldsymbol{x}) = \underset{T_\bullet}{\min} \|T_\bullet(\boldsymbol{x}) - \boldsymbol{\Psi}^*\boldsymbol{\Theta}^*\|_F^2 + \alpha\|\boldsymbol{\Theta}^*\|_0 \end{cases} \tag{7}$$

Here, we note that the orthogonal dictionary $\boldsymbol{\Psi}^H \boldsymbol{\Psi} = \boldsymbol{I}$, where $\boldsymbol{I}$ is the identity matrix. These components are then alternately solved in an iterative fashion, which is illustrated in detail as follows.

3.1 Orthogonal basis learning

The above discussion indicates that one of the subproblems in (7) would be best solved by obtaining the optimal orthogonal basis $\boldsymbol{\Psi}^*$ through a learning approach,

while ensuring that the orthogonal dictionary $\boldsymbol{\Psi}^*$ obtained by iterations is an orthogonal matrix.

Suppose that $\boldsymbol{\Psi}_{t-1}$ and a training dataset $\boldsymbol{x}$ are given initially, after the transformation analysis $\boldsymbol{T}_{\bullet}$ temporarily fixed, the best coefficient vector is obtained approximately as

$$\boldsymbol{\Theta}^* = \boldsymbol{D}_K(\boldsymbol{x}, \boldsymbol{\Psi})\boldsymbol{\Psi}_{t-1}^{\mathrm{H}}\boldsymbol{T}_{\bullet}(\boldsymbol{x}) \qquad (8)$$

where $\boldsymbol{D}_K(\boldsymbol{x}, \boldsymbol{\Psi})$ represents a K-sparse diagonal matrix, which indicates that there are K largest coefficients above zero.

Then, based on the coefficient vector $\boldsymbol{\Theta}^*$ obtained temporarily, we adopt the SVD decomposition for $\boldsymbol{T}_{\bullet}(\boldsymbol{x})\boldsymbol{\Theta}^{*\mathrm{H}}$

$$\begin{cases} \boldsymbol{U\Sigma V}^{\mathrm{H}} = \boldsymbol{T}_{\bullet}(\boldsymbol{x})\boldsymbol{\Theta}^{*H} \\ \boldsymbol{\Psi}_t^* = \boldsymbol{UV}^{\mathrm{H}} \end{cases}. \qquad (9)$$

With the gradient descent algorithm, a few or all of the parameters are adjusted to minimize the output error and the I-SRTD in unrestricted form is conducted by

$$\boldsymbol{\Psi}_{t+1}^* = \boldsymbol{\Psi}_t^* - \alpha\nabla\boldsymbol{J}(\boldsymbol{T}_{\bullet}(\boldsymbol{x}), \boldsymbol{\Psi}_t^*) \qquad (10)$$

where $\nabla\boldsymbol{J}(\boldsymbol{T}_{\bullet}(\boldsymbol{x}), \boldsymbol{\Psi}_t^*)$ is the gradient of the cost function $\boldsymbol{J}(\cdot)$ (also denoted as the estimation error), which can be derived from (10) as follows:

$$\boldsymbol{J}(\boldsymbol{T}_{\bullet}(\boldsymbol{x}), \boldsymbol{\Psi}_t^*) = \left\|\boldsymbol{T}_{\bullet}(\boldsymbol{x}) - \boldsymbol{\Psi}_t^*\boldsymbol{\Theta}^*\right\|_{\mathrm{F}}^2 = \\ \sum_{i=1}^{L}\left\|\boldsymbol{T}_{\bullet}(\boldsymbol{x}_i) - \boldsymbol{\Psi}_t^*\boldsymbol{\Theta}^*(\boldsymbol{T}_{\bullet}(\boldsymbol{x}_i))\right\|_{\mathrm{F}}^2. \qquad (11)$$

Meanwhile, the cost function and its gradient may be obtained further by combining (9) with (11) as follows:

$$\boldsymbol{J}(\boldsymbol{T}_{\bullet}(\boldsymbol{x}), \boldsymbol{\Psi}_t^*) = \|\boldsymbol{T}_{\bullet}(\boldsymbol{x})\|_{\mathrm{F}}^2 - \\ \sum_{i=1}^{L}[\boldsymbol{T}_{\bullet}(\boldsymbol{x}_i)]^{\mathrm{H}}\boldsymbol{\Psi}_t^*\boldsymbol{D}_K(\boldsymbol{x}_i, \boldsymbol{\Psi}_t^*)\cdot\boldsymbol{\Psi}_t^{*\mathrm{H}}\boldsymbol{T}_{\bullet}(\boldsymbol{x}_i), \qquad (12)$$

$$\nabla\boldsymbol{J} = -\boldsymbol{\Psi}_{t-1}^{\mathrm{H}}\hat{\boldsymbol{T}}_{\bullet}(\boldsymbol{x})\hat{\boldsymbol{T}}_{\bullet}(\boldsymbol{x})^{\mathrm{H}}. \qquad (13)$$

Considering the fact that compressive signals are generalized commonly as the exponential form with the increase of α [29], we can adjust the value of α_t iteratively by

$$\alpha_t = \alpha_0 t^{-r}\left(\frac{\alpha_0}{t_{\max}}\right)^{t-1}, \quad t = 1, 2, \cdots, t_{\max} \qquad (14)$$

where α_0 is the initial setting, r is the adjustable parameter and $t_{\max}$ is the maximum of iterations.

The relationship between the bases obtained at successive iterations $\left\|\boldsymbol{\Psi}_{t+1}^*\right\|_2^2 \geqslant \left\|\boldsymbol{\Psi}_t^*\right\|_2^2$ is restricted with an arbitrary $\boldsymbol{x}$ after applying the Gram-Schmidt process for orthogonalization and normalization of the bases. This provides the corresponding restrictions:

$$\boldsymbol{J}(\boldsymbol{T}_{\bullet}(\boldsymbol{x}), \boldsymbol{\Psi}_{t+1}^*) \leqslant \boldsymbol{J}(\boldsymbol{T}_{\bullet}(\boldsymbol{x}), \boldsymbol{\Psi}_t^*). \qquad (15)$$

In this case, the iterative process is continued until the results satisfy the bound $\|\boldsymbol{\Psi}^* - \boldsymbol{\Psi}\|_{\mathrm{F}} \leqslant \varepsilon$, where ε represents an arbitrary parameter of precision.

3.2 Independent transformation analysis

The optimization problem in (11) has been solved based on a number of structured libraries investigated in previous studies, such as time-frequency dictionaries, wavelet packets and cosine packets. Most of these libraries can be considered as corresponding to orthogonal bases in same cases [30]. Herein, we denote these libraries as $\boldsymbol{S}$. An adaptive method for selecting the optimal basis from $\boldsymbol{S}$ [31] is proposed that delivers near-optimal sparsity representations on the order of $N\log_2 N$ in terms of time. This method is formulated as

$$\min \ \boldsymbol{\Xi}\{\boldsymbol{T}_{\bullet}(\boldsymbol{x})\boldsymbol{T}_{\bullet} \subset \boldsymbol{S}\} \qquad (16)$$

where the term $\boldsymbol{\Xi}\{\boldsymbol{T}_{\bullet}(\boldsymbol{x})\} = \sum_i e[\boldsymbol{T}_{\bullet}(\boldsymbol{x}_i)]$ represents the level of entropy associated with information theory and $e[\boldsymbol{T}_{\bullet}(\boldsymbol{x}_i)]$ is an entropy function with scalar representation, which is defined as

$$e[\boldsymbol{T}_{\bullet}(\boldsymbol{x}_i)]_\lambda = \min\left(\|\boldsymbol{T}_{\bullet}(\boldsymbol{x}_i) - \boldsymbol{\Psi}^*\boldsymbol{\Theta}^*\|_{\mathrm{F}}^2 + \alpha\|\boldsymbol{\Theta}^*\|_0, \ \Lambda_i^2\right) \quad (17)$$

where the parameters $\Lambda_i = \lambda^2(1 + t_i)^2$. Here, $\lambda > 0$ is the threshold and $t_i = \sqrt{2\log_2 M_i}$ where M_i represents the total number of distinct vectors occurring among all bases in the library. For example, $M_i = n\log_2 n$ for the structured library based on wavelet packets.

According to the definition of information entropy [32], we can obtain the optimal transformation analysis $\boldsymbol{T}_{\bullet}$ as

$$\boldsymbol{T}_{\bullet}^*(\boldsymbol{x}) = \arg\min \ \boldsymbol{\Xi}\{\boldsymbol{T}_{\bullet}(\boldsymbol{x})\boldsymbol{T}_{\bullet} \subset \boldsymbol{S}\} \qquad (18)$$

where there exists the probability of occurrence exceeding $(1-\varepsilon/M_i)$ when (18) satisfies the condition

$$\left\|\boldsymbol{T}_{\bullet}^*(\boldsymbol{x}) - \boldsymbol{T}_{\bullet}(\boldsymbol{x})\right\|_{\mathrm{F}}^2 \leqslant \frac{\lambda\Lambda_i}{\mathrm{Th} - \lambda}\cdot\min_{\boldsymbol{T}_{\bullet}\subset S} \ \boldsymbol{\Xi}\{\boldsymbol{T}_{\bullet}^*(\boldsymbol{x}) - \boldsymbol{T}_{\bullet}(\boldsymbol{x})\} \qquad (19)$$

where Th is the obtained threshold of the optimal transformation analysis.

The overall processing presents the convergent proper-

ties of the OBL-TA, and it will converge to the global minimum at the end. The iterative process of the OBL-TA algorithm is illustrated in Fig. 2. Above all, we can utilize the effectiveness of the different transform domains to independently obtain the optimal transformation analysis for the corresponding general signal according to the accuracy of sparse approximation based on the obtained orthogonal basis, which will further improve the validity of interference classification and mitigation.
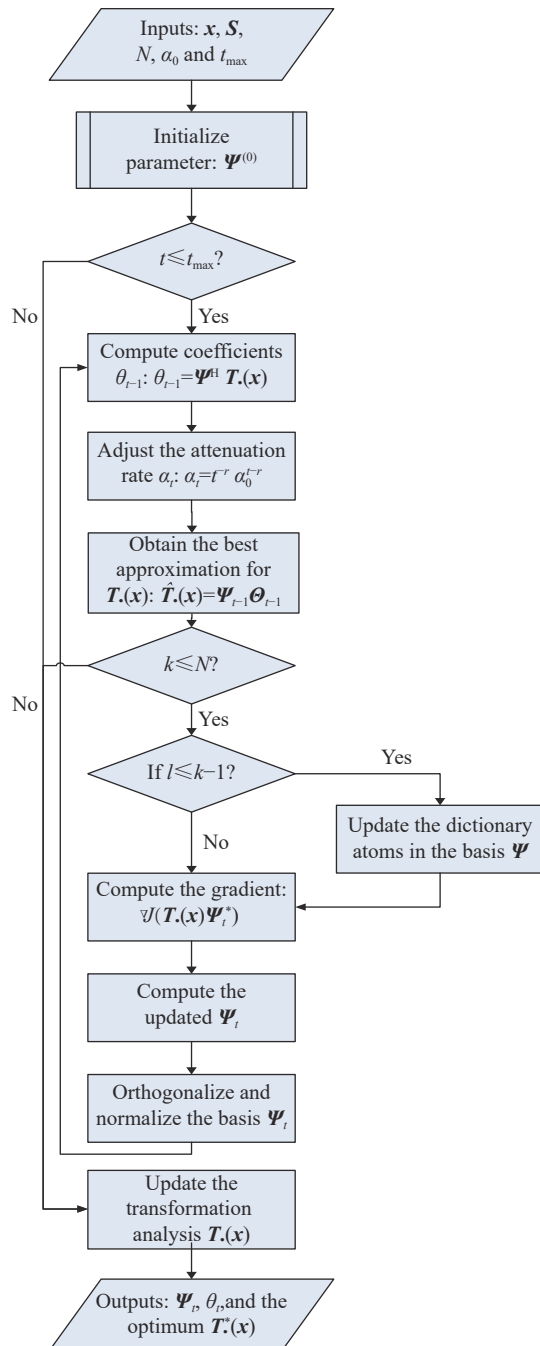

Fig. 2　Iterative process of the OBL-TA algorithm

4. Optimal transformation analysis separately

4.1　Synthesized signal forms

The detection of synthesized signal forms at the receiver is not affected in the spectrum sensing stage of TDCS because its signals are highly sparse and noise-like. Thus, the synthesized form of received signals may be determined by whether the interference exists or not according to the obtained rejection domain in transformation analysis. The problem based on the hypothesis testing is illustrated as

$$y = \begin{cases} H_0 : s + j + n \\ H_1 : s + n \end{cases} \tag{20}$$

where y is the perceived electromagnetic information, s is the TDCS communication signal, j (if it exists) is electromagnetic interference, and n is the environmental noise.

If the assumption H_0 is true, different forms of interference should be considered in this case, such as the narrowband interference and the multi-tone interference. According to the obtained dictionary for signal or interference separately by orthogonal basis leaning, the spectrum estimation with sparse representation in transformed domains may be given by

$$y' = T.(s + j + n) = T.(s) + T.(j) + n' = \Psi_S \theta_S + \Psi_J \theta_J + n' \tag{21}$$

where y' denotes the transformed signal, Ψ_S and Ψ_J are the dictionary of signal and interference, respectively. θ_S and θ_J are the multiple coefficients representing sparsely for signal and interference and n' is a transformed noise vector.

To create a spectrum mask for avoiding the interference more intelligently and accurately, an artificial intelligence (AI)-enabled engine is embedded in TDCS [33]. In clarity, a transmitter is presented in Fig. 3 where the engine consists of three parts, the approximation, classification, and transformation analysis for interference samples. The approximation element is designed for improvement on anti-jamming performance in system, especially under large samples and variable unknown interference. It requires some signal approximation algorithms for restricted different conditions, such as projection theorem and sparse approximation. The classification element is utilized by the intelligent methods (i.e., swarm intelligence, reinforce learning, and neural networks) to distinguish various types whatever the known or unknown

interference is. Furthermore, the transformation analysis aims to find the connotative characteristics of interference, and it makes both the transmitter and receiver mitigate the interference more effectively and specifically.
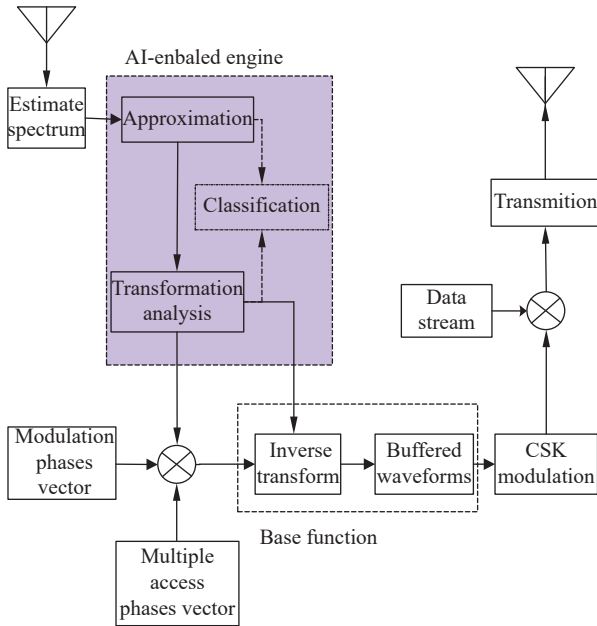

Fig. 3   Modified TDCS transmitter embedded AI-enabled engine

Consequently, the unknown vector $T_.(s)$ and $T_.(j)$ can be represented sparsely in the multiple transform analysis $T_.$. To further determine a sparse object in a transformed domain while reducing residuals due to sparsity constraints alone by means of the total-variation norm [34], the problem can be described as

$$\min_{T} \quad \|T_.(s)+T_.(j)\|_1$$
$$\text{s.t.} \begin{cases} \|s+j\|_{\text{TV}} \leqslant K \\ \|y' - \Psi_S \theta_S + \Psi_J \theta_J\|_{\text{F}} \leqslant \varepsilon \end{cases} \quad (22)$$

where K is the enforcing sparsity of the synthesized forms in some transform, ε is an adjustable scalar and the $\|\cdot\|_{\text{TV}}$ denotes the total-variation norm, which is defined as

$$\|x\|_{\text{TV}} = \sum_{m,n} \sqrt{\left|x_{m+1,n} - x_{m,n}\right|^2 + \left|x_{m,n+1} - x_{m,n}\right|^2}. \quad (23)$$

Based on the assumptions of the separate characteristics for interference and sparse signals in [35], the synthesized form of the problem in (22) for interference is achieved by convex constraints:

$$\min_{T} \|T_.(s)+T_.(j)\|_1 + \lambda\|s+j\|_{\text{TV}}$$
$$\text{s.t.} \quad \|y' - \Psi_S\theta_S + \Psi_J\theta_J\|_{\text{F}} \leqslant \varepsilon. \quad (24)$$

Typically, the parameter ε is adjusted to make the solutions feasible or high probability when the noise is stochastic.

However, most of the works are concerned with the aforementioned unconstrained problem in (5), the similar methods cannot handle important variations in (24) and it requires to be addressed efficiently in practice.

4.2   Optimal selector of transform domain

In this section, we develop an improved method for solving the aforementioned problem by conic alternatives, dualization, and smoothing.

Firstly, due to the generalized transformation analysis $T_.(s)$ and $T_.(j)$ without analytical forms, the conic alternatives are applied to the synthesized forms in (24), which is represented as

$$\min z + \lambda\|s+j\|_{\text{TV}}$$
$$\text{s.t.} \begin{cases} \|T_.(s)+T_.(j)\|_1 \leqslant z \\ \|y' - \Psi_S\theta_S + \Psi_J\theta_J\|_{\text{F}} \leqslant \varepsilon \end{cases} \quad (25)$$

where z is a new introduced variable.

Similarly, the total-variation norm $\|x\|_{\text{TV}}$ can be cast as a complex l_1-norm problem $\|W(x)\|_1$, where $W(\cdot)$ represents as the linear operation for x and it is defined as

$$[W(x_{m,n})] = (x_{m+1,n} - x_{m,n}) + \text{j}(x_{m,n+1} - x_{m,n}). \quad (26)$$

Therefore, the transformed forms of conic alternatives can be derived from (25):

$$\min \quad z + \lambda t$$
$$\text{s.t.} \begin{cases} \|T_.(s)+T_.(j)\|_1 \leqslant z \\ \|W(s+j)\|_1 \leqslant t \\ \|y' - \Psi_S\theta_S + \Psi_J\theta_J\|_{\text{F}} \leqslant \varepsilon \end{cases} \quad . \quad (27)$$

Then, the dual variables (p_1, p_2, p_3) compose the Lagrangian forms, which is given by

$$L(s,j;p_1,p_2,p_3) = -\langle p_1, T_.(s) + T_.(j)\rangle - \\ \langle p_2, W(s+j)\rangle - \langle p_3, y' - \Psi_S\theta_S + \Psi_J\theta_J\rangle - \varepsilon\|p_3\|_{\text{F}} \quad (28)$$

where $\langle\cdot\rangle$ represents the inner product.

Because the cost function may be not differentiable on some points, a smoothing approach [36] is utilized to approximate the problem in (27) and the dual function may be demonstrated as

$$g_u(p_1, p_2, p_3) = \inf_x \frac{1}{2} u \|s + j - x_0\|_F^2 - \langle p_1, T.(s) + T.(j) \rangle -$$

$$\langle p_2, W(s+j) \rangle - \langle p_3, y' - \Psi_S \theta_S + \Psi_J \theta_J \rangle - \varepsilon \|p_3\|_F \quad (29)$$

where x_0 means a feasible solution. Ultimately, the minimum can be obtained:

$$x(s, j; p) = x_0 + u^{-1} \left[T.^{-1}(p_1) + W^{-1}(p_2) - \right.$$

$$\left. (\Psi_S \theta_S + \Psi_J \theta_J) p_3 \right]. \quad (30)$$

To achieve convergence of dual projection certainly, different iterative steps $t^{(k)}$ are applied to each dual variables, which is given by

$$p^{(k+1)} = \arg\min_p \varepsilon \|p_3\|_F + \langle \hat{x}, p \rangle +$$

$$\frac{t^{(k)} a^{(k)}}{2} \cdot \|p - p^{(k)}\|_F^2 \quad (31)$$

where $\hat{x} = (T.(s) + T.(j), W(s+j), y' - \Psi_S \theta_S + \Psi_J \theta_J)$.

Finally, the feasible solutions [37] are obtained by

$$\begin{cases} p_1^{(k+1)} = \mathrm{Trc}\left({y'_1}^{(k)} - \frac{t_1^{(k)} \hat{x}_1}{\alpha^{(k)}}, \frac{\hat{x}_1}{\alpha^{(k)}} \right) \\ p_2^{(k+1)} = \mathrm{CTrc}\left({y'_2}^{(k)} - \frac{t_2^{(k)} \hat{x}_2}{\alpha^{(k)}}, \frac{\hat{x}_2}{\alpha^{(k)}} \right) \\ p_3^{(k+1)} = \mathrm{Shk}\left({y'_3}^{(k)} - \frac{t_3^{(k)} \hat{x}_3}{\alpha^{(k)}}, \frac{\hat{x}_3 \varepsilon}{\alpha^{(k)}} \right) \end{cases} \quad (32)$$

where $\mathrm{Trc}(a,b)$ and $\mathrm{CTrc}(a,b)$ represent the element-wise truncation operators, and $\mathrm{Shk}(a,b)$ is an l_2-shrinkage operation, which are defined as

$$\begin{cases} \mathrm{Trc}(a,b) = \mathrm{sgn}(a) \cdot \min\{|a|, b\} \\ \mathrm{CTrc}(a,b) = \min\left\{ 1, \frac{b}{|a|} \right\} \\ \mathrm{Shk}(a,b) = a \cdot \max\left\{ 1 - \frac{b}{\|a\|_F}, 0 \right\} \end{cases} \quad . \quad (33)$$

Fig. 4 below depicts a standard continuation loop for solving the problem of OPTAS and it will converge to the global minimum at the end. Above all, we can utilize the effectiveness of the different transform domains to separately obtain the optimal transformation analysis for the corresponding synthesized signal forms according to the accuracy of sparse approximation based on the obtained optimal selector, which will further improve the validity of interference separation and elimination.
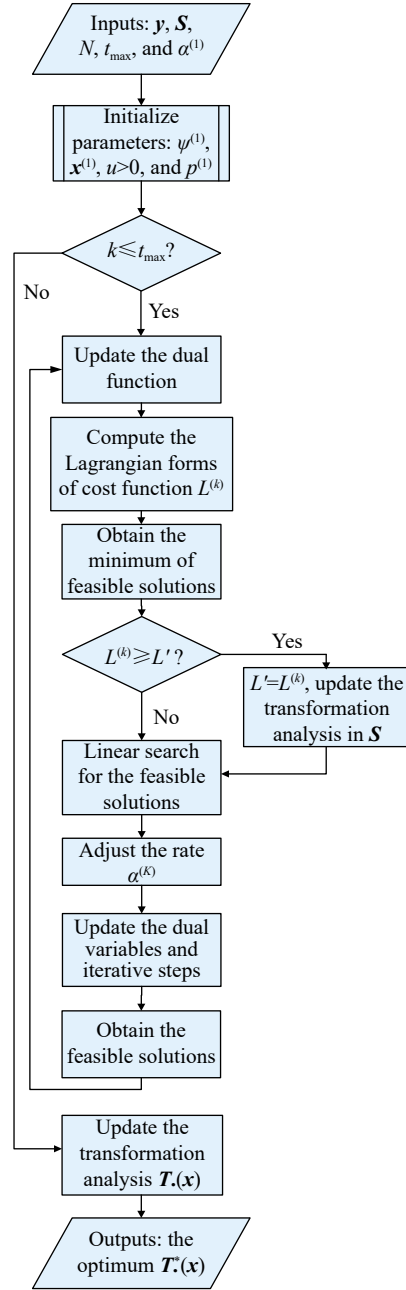

Fig. 4   Iterative loop for solving the problem by OPTAS algorithm

5. Simulation results and discussion

The effectiveness of the proposed OBL-TA method is verified generally by conducting experiments with datasets of sparse signals with variable but limited sparsity levels and general sparse signals. Then the results are compared with orthogonal sparse coding (OSC) and its derivative geodesic flow OSC (GF-OSC) for sparse representation [14]. The number of sampling points for interference signals is employed as 1 024 and the signal to noise ratio is 8 dB where the noise is assumed to be a Gaussian white noise channel. For detailed parameters,

the representative interference signals are selected with distinct sparsity including multi-tone interference, chirp interference, comb-spectrum interference and frequency modulation for noise interference signals. Here, single-tone interference samples are considered based on generated sine waves. The detailed characteristics of the types of interference datasets are listed in Table 1. The sparsity level of the interference signals is adjusted randomly in the scale of [5,30]. The performances of the methods are evaluated in terms of the measured degree of sparsity, the convergence behaviour, comparisons of performance and the impact of system performance. Additionally, the optimal transformation analysis performance obtained by the proposed OPTAS method is compared with that obtained by the FFT, FrFT, DCT, and DWT domains for a selection of the interference signals, which is listed in Table 1.

Table 1 Characteristics of interference datasets

Interference type	Frequency	Bandwidth	Amplitude
Multi-tone	Constant	Constant	Random
Comb-spectrum	Regular	Constant	Regular
Chirp	Regular	Regular	Constant
Frequency modulation for noise	Regular	Regular	Constant

5.1 General transformation analysis

In this subsection, various interference signals are tested as examples and their sparsity levels are variable but unknown. A wideband spectrum sensing method [30] is utilized to measure the sparsity of interference signals. Generally, compressed sensing is employed to acquire the sensed interference signal from the datasets at sub-Nyquist rates and the sums of the frequency components are estimated by least squares optimization. The sparsity is assumed as the total number of frequency subbands based on hypothesis testing for the average detection probability. Among them, single-tone interference, multi-tone interference and partial-band interference signals are above 60 in sparsity whereas impulse interference, comb-spectrum interference and frequency modulation for noise interference signals are below 40. Besides, the amplitude modulation for noise interference and chirp interference signals are in between.

Fig. 5 presents the relative estimation error obtained at each iteration epoch of the I-SRTD for a selection of interference signals with varying levels of sparsity.

(a) Multi-tone interference

(b) Chirp interference

(c) Comb-spectrum interference

(d) Frequency modulation for noise interference

: 5; : 10; : 15; : 20; : 25; : 30.
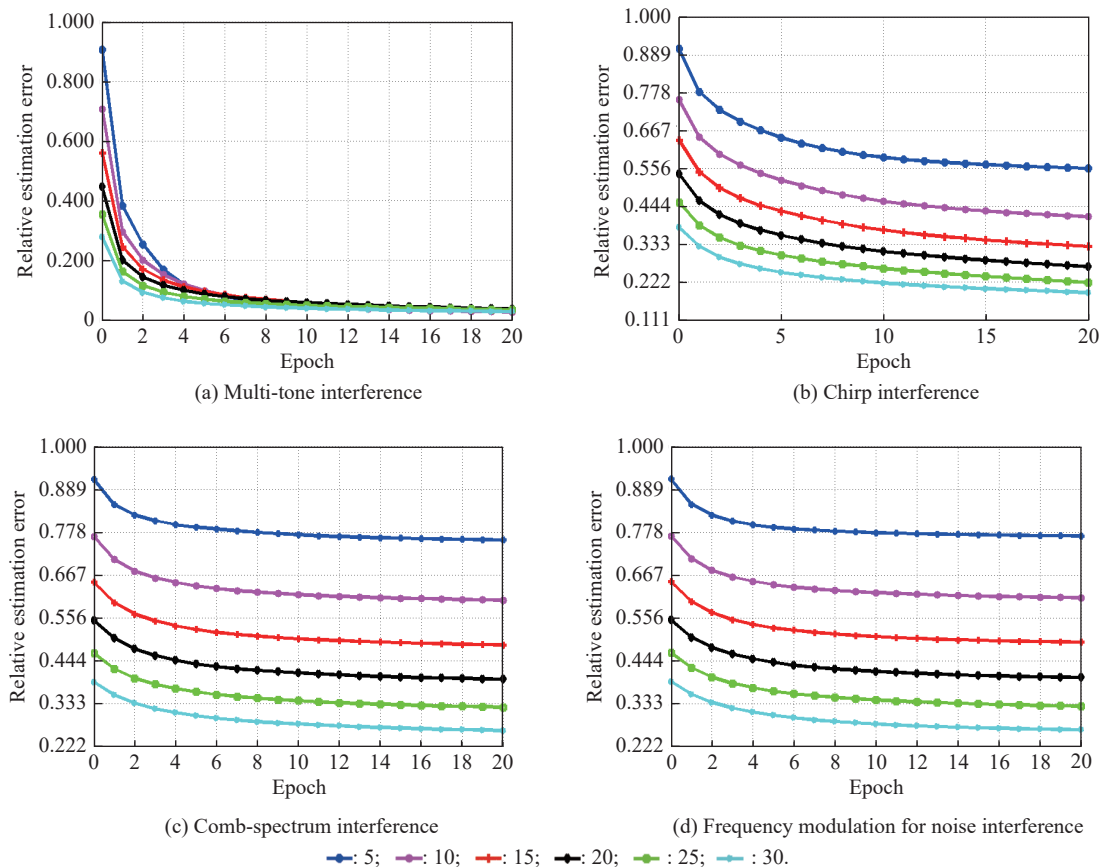
Fig. 5   Relative estimation errors obtained by I-SRTD as a function of iteration epochs for a selection of interference signals of known sparsity

The results indicate that the relative estimation error decreases rapidly initially and then slowly with increasing iterations for all interference types considered above, in interference type from steep to steady almost, even for comb-spectrum interference and frequency modulation for noise interference types. In addition, the relative estimation error generally decreases with increasing sparsity. The conclusion is drawn that the higher the levels of sparsity, the better effectiveness of sparse representation for interference signals. However, increasing sparsity can interfere with the recovery of interference signals. Furthermore, the level of sparsity affects the representation of interference signals variously, and we can achieve the optimal representation by the transformation analysis even the level of sparsity remains a relatively low level. Consequently, the optimal transformation analysis based on the unknown sparsity of interference signals is in greater need, and our proposed OBL-TA method is suited for these applications more ideally.

For further verfying the convergence behavior of the OBL-TA algorithm and its adaptability for various interferece, some comparisons are conducted in this subsection. Among them, the length of received signals $L = 1\,024$, each containing 20 spikes created by choosing 20 locations at random and then putting 0 at these points. Accordingly, the sparsity of the signals is 2, but all have random amplitudes. The projection matrix is constructed by first creating a matrix with a Gaussian distribution and normalizing the rows of the matrix to a unit value. Gaussian white noise is added to the given datasets when the signal to noise ratio is 8 dB and the transformation analysis is implemented using OBL-TA, OSC, and GF-OSC, respectively.

Fig. 6 presents the relative estimation errors obtained with respect to iteration epochs when applying the above algorithms to the same interference signals.
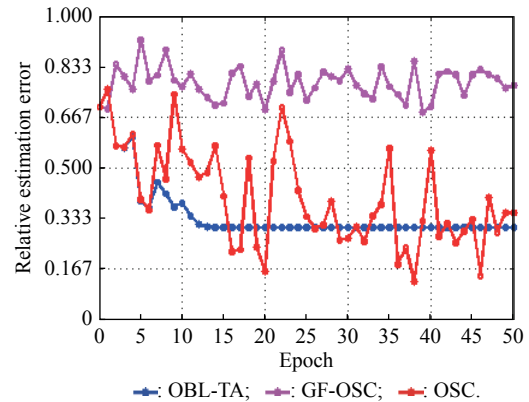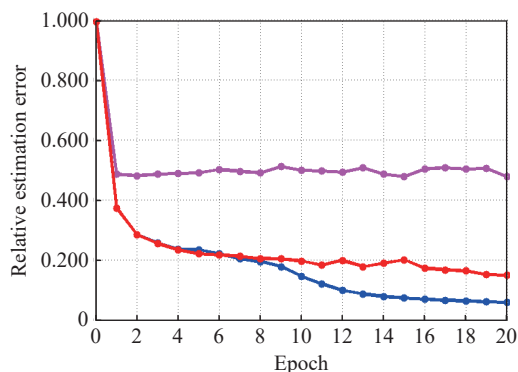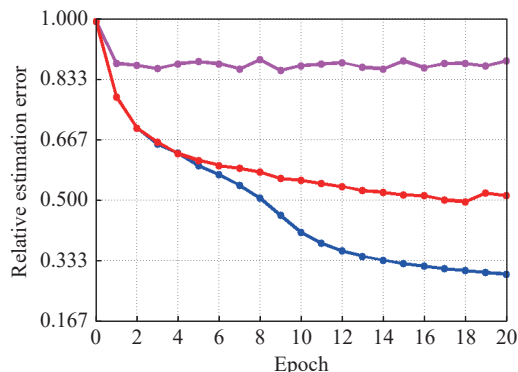

Fig. 6 Relative estimation errors obtained with respect to iteration epochs when applying the OBL-TA, GF-OSC, and classical OSC algorithms to the same interference signals

It is noted that the relative estimation errors of the optimal orthogonal basis obtained by OBL-TA decrease gradually and rapidly converge to the best sparse representation under the corresponding transform domains while the convergence is not as readily discernible for the OSC and GF-OSC algorithms and their estimation errors are greater. Obviously, the proposed OBL-TA achieves convergence rapidly and obtains less relative estimation errors, which provides superior sparse representation performance relative to that of the other two algorithms considered.

More generally applicable results are presented in Fig. 7, which presents the relative estimation errors obtained with respect to iteration epochs when applying the OBL-TA, GF-OSC, and OSC algorithms to a selection of the interference signals listed in Table 1 with unknown sparsity, but the level of sparsity randomly changes in the given scope of [20,80]. It is noted that the proposed method improves the representation accuracy in the range of 25%−40% relative to those of the other methods in whole, and the improvement is about 50% for frequency modulation for noise interference signals. Additionally, due to the levels of sparsity are arranged in order from the higher to the lower, the relative estimation errors are gradually descending with the increasing levels of sparsity.

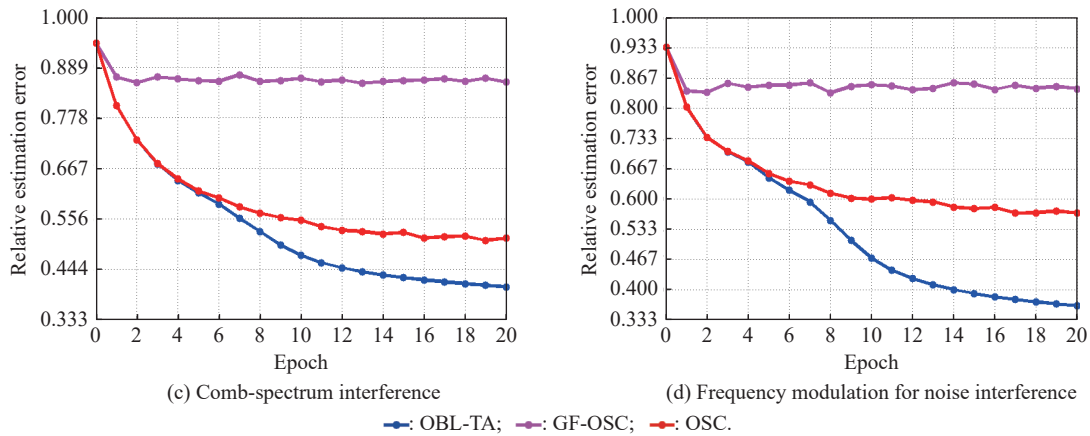(a) Multi-tone interference

(b) Chirp interference

(c) Comb-spectrum interference

(d) Frequency modulation for noise interference

—•—: OBL-TA;   —•—: GF-OSC;   —•—: OSC.

Fig. 7   Relative estimation errors obtained with respect to iteration epochs when applying the OBL-TA, GF-OSC, and OSC algorithms to a selection of the interference signals with unknown sparsity

5.2   Optimal transform analysis

Fig. 8 presents the relative estimation errors obtained for multi-tone interference (Signal I), chirp interference (Signal II), comb-spectrum interference (Signal III), and frequency modulation for noise interference (Signal IV) in the FFT, FrFT, DCT, or DWT domains. And the levels of sparsity are arranged in order from the higher to the lower of the scope 60−80, 50−60, 40−50, and 20−40, respectively. Here, the level of the entropy function is obtained by the convergent value in the libraries of transform domains and the optimal transformation analysis is obtained by the OPTAS method.
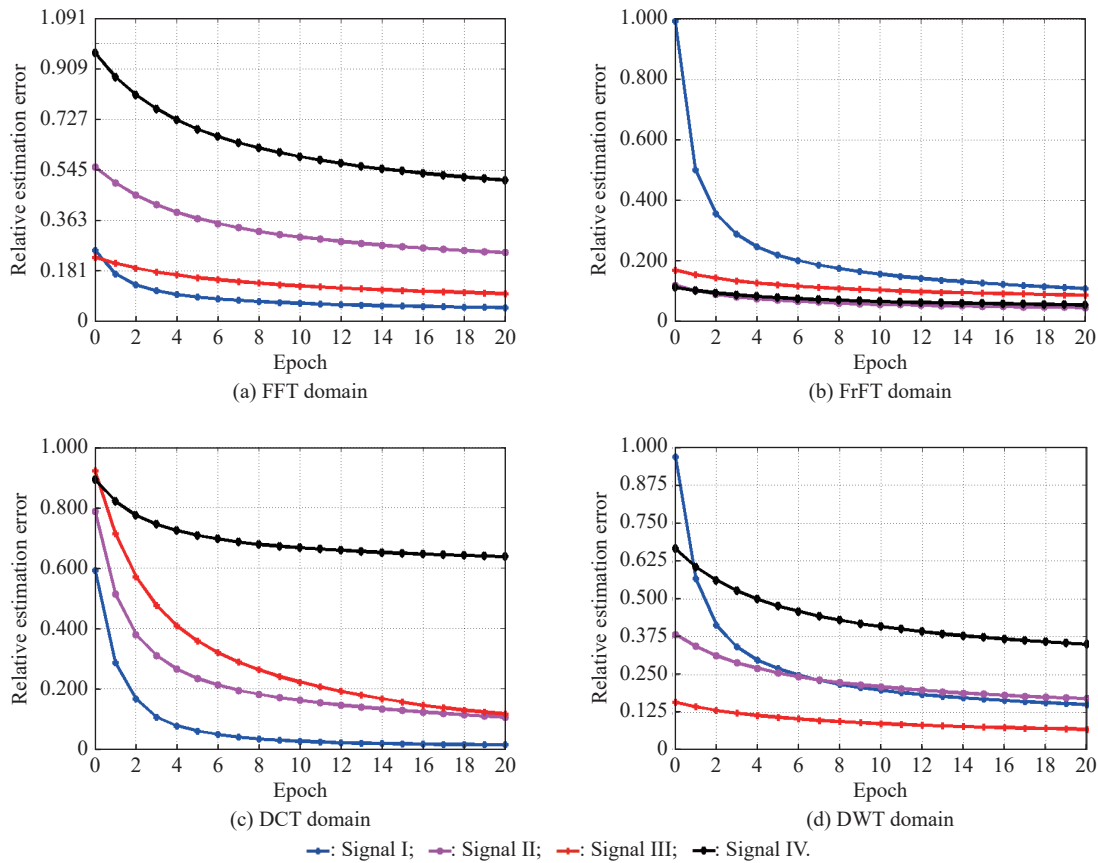

(a) FFT domain

(b) FrFT domain

(c) DCT domain

(d) DWT domain

—•—: Signal I;   —•—: Signal II;   —•—: Signal III;   —•—: Signal IV.

Fig. 8   Relative estimation errors obtained for multi-tone interference (Signal I), chirp interference (Signal II), comb-spectrum interference (Signal III), and frequency modulation for noise interference (Signal IV) in different domains

These results demonstrate that different types of interference signals are particular well processed in different domains. For example, it is noted that multi-tone interference signals with higher sparsity are well suited for the simple FFT and DCT domains, whereas the frequency modulation for noise interference signals with lower sparsity is well suited for the complex FrFT domain. This is because that the representation of high-sparse interference signals is easier than that of low-sparse interference signals, the sparse separability can be utilized to distinguish sharply from the different sparse interference signals by the particular transform domain.

Meanwhile, the time-sensitive evaluation is required for the proposed OPTAS method. For four groups of interference signals with the change of frequency, 20 Monte-Carlo simulations are executed and the sampling frequency f_s=1 024 MHz. The channel is assumed to be a Gaussian white noise channel when the signal to noise ratio is within the scope of 6 dB to 10 dB. All experiments are performed in the Matlab R2013b environment and the simulation hardware platform is an Intel(R) Core(TM) i7 CPU (3.40 GHz), 4G memory PC. Here, the timely accuracy ratio is defined as TAR= accuracy/time and relative TAR of transformation analysis RTAR= TAR/TAR$_{max}$ where TAR$_{max}$ represents the maximum of the timely accuracy ratios under different transform domains. Both of them reflect the time-sensitive evaluation for interference signals under transformation analysis in some degree. The relative running time ratios consumed for different interference signals in the FFT, FrFT, DCT, and DWT domains are presented in Fig. 9.
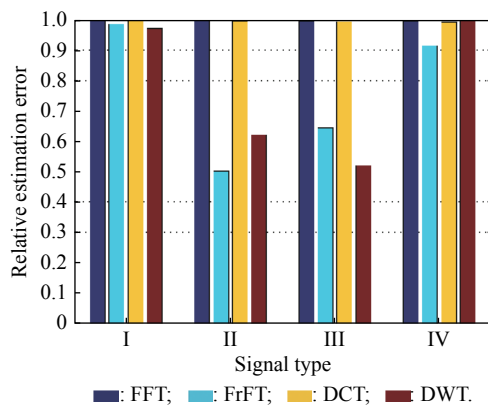

Fig. 9　Relative running time ratios consumed for different interference signals in the FFT, FrFT, DCT, and DWT domains

The results illustrate that the different transform domains are particular well suited to different types of interference signals and have great difference in processing time-effectiveness. For example, the relative running time ratios of multi-tone interference signals under the FFT, FrFT, DCT, and DWT domains are similar to each other whereas the FFT and DCT domains are simpler than the others. In contrast, the relative running time ratios of chirp interference and comb-spectrum interference signals under the FrFT and DWT domains are more efficient than that of FFT and DCT domains due to the time-varying and complex characteristics required for detailed analysis.

5.3 Performance analysis for diverse spectrum states

When a TDCS system is put into the complex electromagnetic environment, the transmitter and the receiver will be situated in different spectrum states and their states can be divided into the consistency and inconsistency with spectrum sensing, which results in the diversity of interference processing.

To further exploit the impact factors on the performance of bit-error-rate (BER) for addressing different interferences by the OPTAS method, multi-tone interference (Signal I) and comb-spectrum interference (Signal III) are selected in the consistent spectrum sensing cases. The variable spectrum dataset of measured interference is determined by the settings in Table 1, where the frequency range of Signal I varies from [30,55,85] kHz to [280,305,335] kHz and the adjustable rate range of Signal III interference varies from 130 to 380, and the frequency range varies from 80 kHz to 330 kHz. For the interference and noise power, the initial signal to noise ratio is 4 dB where the noise is assumed to be a Gaussian white noise channel. Moreover, all interferences to noise ratios (INRs) change from −4 dB to 10 dB with the interval of 1 dB where the noise power is constant. The experiment results for different sparse interferences in the consistent spectrum sensing cases are illustrated in Fig. 10.
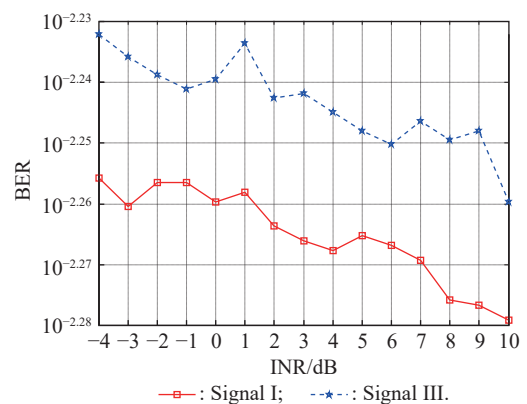

Fig. 10　Comparison of BER obtained for multi-tone interference (Signal I) and comb-spectrum interference (Signal III) in the consistent spectrum sensing

It is demonstrated that the mitigation performance of multi-tone interference and comb-spectrum interference are improved gradually with the increase of the INRs, which indicates the higher power density of interference is more available for separation. However, when the INRs of the comb-spectrum interference keep in the degree of −2 dB to 2 dB, its BERs performance makes worsen than others for its similarity to the noise. Distinctly, it takes the advantage for addressing multi-tone interference when compared with that of comb-spectrum interference due to the intrinsic complexity in spectrum distribution.

The next section of the experiment is conducted for the demodulation performance of BERs for TDCS signals in the inconsistent spectrum sensing cases. For traditional TDCS system, it is a tough task to settle this different spectrum cases due to the interaction between the transmitter and receiver for synthesizing the base function. When the detection error is obtained by sensing spectrum in the receiver, the performance will degrade obviously [38]. Thus, the BERs performance for traditional TDCS and the proposed AI-enabled TDCS in Section 4 are compared in Fig. 11. Here, the detection error is simplified as the difference of sensed spectrum between the receiver and transmitter. It is known that the most accredited degree of detection error for keeping communication is about 25% and this complex spectrum case is selected as the sample. The mean values of BER from 100 simulations are adopted as the final result and the interference parameters are set as same as those in Fig. 10. Meanwhile, the comb-spectrum interference is selected as the representative interference.
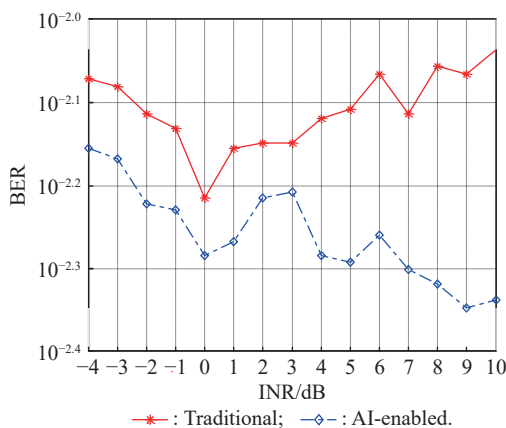
Fig. 11　Comparison of the BERs performance obtained for interference mitigation among the traditional TDCS and the proposed AI-enabled TDCS when the sensed spectrum is inconsistent

The results illustrate that the BER of the proposed AI-enabled TDCS is more acceptable than the traditional TDCS for its flexible separation of interference spectrum. It is evident that the performance degraded gradually with the increase of INRs. The reason for the poor interference mitigation performance is that the accumulated error for signal separation is not satisfactory when the interference power makes bitter. Furthermore, the ideal results are found that the impacts of interference on the proposed AI-enabled TDCS are suppressed more clearly than the conventional whereas both of them are suited for low power interference almost below 0 dB. As the power density of interference grew higher above 3 dB, the proposed AI-enabled TDCS achieves smaller BERs and descending tendency when compared with the traditional TDCS of up-growing BERs, which demonstrates its superiority in interference mitigation.

6. Conclusions

The optimal transformation of interference is an important factor restricting the anti-jamming performance of TDCSs for tactical communication. In this paper, an OBL-TA is proposed based on sparse representation. Sparse availability is utilized to obtain the optimal transformation analysis by the SRTD in unrestricted form. In addition, the I-SRTD in unrestricted form is obtained by decomposing the SRTD problem into learning the best orthogonal basis. Furthermore, based on the assumptions of the separate characteristics for interference and sparse signals, an OPTAS is applied to the synthesized signal forms with conic alternatives, dualization, and smoothing. The process enables us to utilize the effectiveness of different transform domains to obtain the optimal transformation analysis according to the accuracy of sparse representation based on the obtained orthogonal basis, which will further improve the validity of interference classification and mitigation. The simulation results demonstrate that the proposed method obtain the optimal transform domain more rapidly and accurately than conventional methods, and it can therefore effectively meet the requirements of interference classification and mitigation, which significantly improves the anti-jamming performance of TDCSs.

References

[1] HU S, GUAN Y L, BI G A, et al. Cluster-based transform domain communication systems for high spectrum efficiency. IET Communications, 2012, 6(16): 2734–2739.

[2] FUMAT G, CHARGE P, ZOUBIR A, et al. Using set theoretic estimation to address the PAPR problem of spectrum-constrained signals. IEEE Trans. on Wireless Communications, 2012, 11(7): 2373–2381.

[3] HU S, BI G A, GUAN Y L, et al. TDCS-based cognitive radio networks with multiuser interference avoidance. IEEE Trans. on Communications, 2013, 61(12): 4828–4835.

[4] FUMAT G, CHARGE P, ZOUBIR A, et al. Transform

domain communication systems from a multidimensional perspective: impacts on bit error rate and spectrum efficiency. IET Communications, 2010, 5(4): 476–483.

[5] LIN R, BI G A, LIU X, et al. On the modulation and signaling design for a transform domain communication system. IET Communications, 2014, 8(16): 2909–2916.

[6] CHAKRAVARTHY V, NUNEZ A S, STEPHENS J P, et al. TDCS, OFDM, and MC-CDMA: a brief tutorial. IEEE Communications Magazine, 2005, 43(9): S11−S16.

[7] SUN D C, CHEN Y, LIU J A, et al. Digital signal modulation recognition algorithm based on VGGNet model. Proc. of the IEEE 5th International Conference on Computer and Communications, 2019: 1575–1579.

[8] YANG Z Y, TAO R, WANG Y, et al. A novel multi-carrier order division multi-access communication system based on TDCS with fractional Fourier transform scheme. Wireless Personal Communications, 2014, 79(2): 301–320.

[9] WANG G S, WANG Y Q, HUANG G C, et al. Classification methods with signal approximation for unknown interference. IEEE Access, 2020, 8: 37933–37945.

[10] KIRBY M, SIROVICH L. Application of the Karhunen-Loeve procedure for the characterization of human faces. IEEE Trans. on Pattern Analysis & Machine Intelligence, 1990, 12(1): 103–108.

[11] FRALEY C, RAFTERY A E. Model-based clustering, discriminant analysis, and density estimation. Journal of American Statistical Association, 2002, 97(458): 611–631.

[12] HE R, ZHENG W S, HU B G, et al. Two-stage nonnegative sparse representation for large-scale face recognition. IEEE Trans. on Neural Networks & Learning Systems, 2013, 24(1): 35–46.

[13] WRIGHT J, YANG A Y, GANESH A, et al. Robust face recognition via sparse representation. IEEE Trans. on Pattern Analysis & Machine Intelligence, 2009, 31(2): 210–227.

[14] SCHIITZE H, BARTH E, MARTINETZ T. Learning efficient data representations with orthogonal sparse coding. IEEE Trans. on Computational Imaging, 2016, 2(3): 177–189.

[15] LEWICKI M. Efficient coding of natural sounds. Nature Neuroscience, 2002, 5(3): 356–363.

[16] TAN X P, SU S J, SUN X Y. Research on narrowband interference suppression technology of UAV network based on spread spectrum communication. Proc. of the IEEE International Conference on Artificial Intelligence and Information Systems, 2020: 335–338.

[17] TENGSTRAND S, ELIARDSSON P, AXELL E. Mitigation of multiple impulse noise sources through selective attenuation. Proc. of the IEEE Military Communications Conference, 2016: 855–860.

[18] KARAWAS G, GOVERDHANAM K, KOH J. Wideband active interference cancellation techniques for military applications. Proc. of the 5th European Conference on Antennas & Propagation, 2011: 390–392.

[19] LIU S C, YANG F, DING W B, et al. Double kill: compressive-sensing-based narrow-band interference and impulsive noise mitigation for vehicular communications. IEEE Trans. on Vehicular Technology, 2016, 65(7): 5099–5111.

[20] YANG J W, LAMARE R C. Widely-linear minimum-mean-squared error multiple-candidate successive interference cancellation for multiple access interference and jamming suppression in direct-sequence code-division multiple-access systems. IET Signal Processing, 2015, 9(1): 73–81.

[21] ZHANG Y, JIA X S, KOU B H. Adaptive multi-tone jam-

ming suppression for DSSS communications based on compressive sensing. Proc. of the 8th International Congress on Image & Signal Processing, 2015: 1323–1327.

[22] AXELL E, ELIARDSSON P, TENGSTRAND S, et al. Power control in interference channels with class A impulse noise. IEEE Trans. on Wireless Communications Letters, 2017, 6(1): 102–105.

[23] CHEN S X, DENG Z D, MA S Q, et al. Manifold proximal point algorithms for dual principal component pursuit and orthogonal dictionary learning. IEEE Trans. on Signal Processing, 2021, 69(7): 4759–4773.

[24] WEI D X, ZHANG S D, CHEN S Q, et al. Research on anti-jamming technology of chaotic composite short range detection system based on underdetermined signal separation and spectral analysis. IEEE Access, 2019, 7: 42298–42308.

[25] SU D T, GAO M G. Research on jamming recognition technology based on characteristic parameters. Proc. of the IEEE 5th International Conference on Signal & Image Processing, 2020: 303–307.

[26] KUZOVNIKOV A. Study of the methods for developing jamming-immune communications systems with the use of wavelet-modulated signals. Journal of Communications Technology & Electronics, 2014, 59(1): 61–70.

[27] DONG Y P, LIAO F Z, PANG T Y, et al. Boosting adversarial attacks with momentum. Proc. of the IEEE/CVF Conference on Computer Vision & Pattern Recognition, 2018: 9185–9193.

[28] WU Y, WANG C, ZHANG Y Q, et al. Unsupervised feature selection via joint local learning and group sparse regression. Frontiers of Information Technology & Electronic Engineering, 2019, 20(5): 538–553.

[29] ELDAR Y, KUTYNIOK G. Compressed sensing: theory and applications. London: Cambridge University Press, 2012.

[30] SHABAN M, PERKINS D, BAYOUMI M. Application of compressed sensing in wideband cognitive radios when sparsity is unknown. Proc. of the 15th Annual IEEE Wireless & Microwave Technology Conference, 2014. DOI: 10.1109/WAMICON.2014.6857771.

[31] COIFMAN R R, WICKERHAUSER M V. Entropy-based algorithms for best-basis selection. IEEE Trans. on Information Theory, 1992, 38(2): 713–718.

[32] DONOHO D L. Adaptive signal representations: how much is too much? Proc. of the Workshop on Information Theory & Statistics, 1994: 53–60.

[33] WANG Y Q, WANG G S, LI N, et al. Cognitive anti-interference communication of unmanned autonomous system supported by intelligent "cloud brain". Proc. of the International Conference on Artificial Intelligence & Computer Engineering, 2020: 199–203.

[34] CANDES E J, GUO F. New multiscale transforms, minimum total-variation synthesis: applications to edge-preserving image reconstruction. Signal Processing, 2002, 82(11): 1519–1543.

[35] ZHANG Y S, JIA X, YIN C B, et al. NBI mitigation in DSSS communications via block sparse Bayesian learning. Signal Processing, 2019, 158(5): 129–140.

[36] NESTEROV Y. Smooth minimization of non-smooth functions. Mathematical Programming: Series A, 2005, 103(12): 127–152.

[37] BECKER S, CANDES, E J, GRANT M. Templates for convex cone problems with applications to sparse signal recovery. Mathematical Programming Computation, 2010, 3(7): 165–218.

[38] HU S, BI G A, GUAN Y L, et al. Spectrally efficient trans-

form domain communication system with quadrature cyclic code shift keying. IET Communications, 2013, 7(4): 382–390.

Biographies

WANG Guisheng was born in 1979. He received his M.S. degree in military communication from the Information and Navigation College, Air Force Engineering University, Xi'an, China, in 2018, where he is currently pursuing his Ph.D. degree in information and communication engineering. He is an engineer in the National Key Laboratory of Airspace Technology. His research interests include compressive sensing based anti-jamming and military aeronautical and cognitive communication.
E-mail: wgsfuyun@163.com

WANG Yequn was born in 1985. He received his M.S. and Ph.D. degrees from Air Force Engineering University in 2009 and 2012, respectively, where he is a currently a lecturer with the Information and Navigation College. His main research interests include aeronautical communication, ad hoc networks, satellite, and high frequency communication.
E-mail: kgdwyq@126.com

DONG Shufu was born in 1970. He received his M.S. degree from Air Force Engineering University, in 1997, and his Ph.D. degree from Xi'an Institute of Optics and Precision Mechanics, Chinese Academy of Sciences, Xi'an, China, in 2005. He is currently a professor with the Information and Navigation College, Air Force Engineering University. His main research interests include aeronautical and communication networking.
E-mail: kgddsf@126.com

HUANG Guoce was born in 1962. He received his M.S. degree from Air Force Telecommunication Engineering College, Xi'an, China, in 1990. He is currently a doctoral supervisor and a professor with the Information and Navigation College, Air Force Engineering University. His main research interests include high frequency communication, aeronautical communication, and satellite communication.
E-mail: kgdhgc@126.com